ATM-mediated phosphorylation of SOG1 is essential for the DNA damage response in *Arabidopsis*

Kaoru Okamoto Yoshiyama[1,2+], Junya Kobayashi[3], Nobuo Ogita[1], Minako Ueda[1], Seisuke Kimura[2], Hisaji Maki[1], Masaaki Umeda[1,4+]

[1]Graduate School of Biological Sciences, Nara Institute of Science and Technology, 8916-5 Takayama, Ikoma, Nara 630-0192, Japan

[2]Department of Bioresource and Environmental Sciences, Kyoto Sangyo University, Kamigamo-Motoyama, Kitaku, Kyoto 603-8555, Japan

[3]Radiation Biology Center, Kyoto University, Yoshida-Konoe, Sakyoku, Kyoto 606-8501, Japan

[4]JST, CREST, 8916-5 Takayama, Ikoma, Nara 630-0192, Japan

[+]Corresponding author

Kaoru O. Yoshiyama, Department of Bioresource and Environmental Sciences, Kyoto Sangyo University, Kamigamo-Motoyama, Kitaku, Kyoto 603-8555, Japan

Tel: +81-75-705-3236; Fax: +81-75-705-1914

E-mail: kaoru.o@cc.kyoto-su.ac.jp

Masaaki Umeda, Graduate School of Biological Sciences, Nara Institute of Science and Technology, 8916-5 Takayama, Ikoma, Nara 630-0192, Japan

Tel: +81-743-72-5592; Fax: +81-743-72-5599

E-mail: mumeda@bs.naist.jp

Running title: ATM-mediated phosphorylation of SOG1

Keywords: DNA damage, *Arabidopsis*, SOG1, p53, phosphorylation, ATM

Total character count: 26,040

ABSTRACT

Arabidopsis SOG1 (suppressor of gamma response 1) is a plant-specific transcription factor that governs the DNA damage response. Here we report that SOG1 is phosphorylated in response to DNA damage, and that this phosphorylation is mediated by the sensor kinase ATM. We show that SOG1 phosphorylation is crucial for the response to DNA damage, including transcriptional induction of downstream genes, transient arrest of cell division, and programmed cell death. Although the amino acid sequences of SOG1 and the mammalian tumor suppressor p53 display no similarity, this study demonstrates that ATM-mediated phosphorylation of a transcription factor plays a pivotal role in the DNA damage response in both plants and mammals.

INTRODUCTION

Chromosomal DNA constantly suffers many types of damage caused by the action of exogenous agents such as ionizing radiation, UV and chemical mutagens, or by cellular metabolism, which produces reactive radicals and stalled replication forks. In response to DNA damage, eukaryotic cells activate signaling pathways that stimulate DNA repair, cell cycle checkpoints, and eventually apoptosis; these events are critical for the maintenance of genome integrity [1]. In mammals, DNA damage is sensed by two protein kinases, ataxia telangiectasia mutated (ATM) and ATM and Rad3-related (ATR), which belong to the phosphatidylinositol 3-kinase family [2]. Each is activated in response to different types of DNA damage: ATM responds to double-strand breaks (DSBs), while ATR mainly responds to single-strand DNA and stalled replication forks [3, 4]. Checkpoint kinases 1 and 2 (CHK1, CHK2) are key signal transducers working downstream of ATR and ATM, respectively, and p53 transcription factor is another crucial downstream factor controlling DNA repair, cell cycle arrest, senescence and apoptosis [5, 6].

Arabidopsis also possesses *ATM* and *ATR* orthologs, which are not essential under non-stressed conditions, although *atm* knockout mutants display partial sterility [7, 8]. This is in marked contrast to mammalian *ATR,* whose disruption induces embryonic lethality [9]. In *Arabidopsis*, *atm* and *atr* mutants are hypersensitive to DSB-inducing agents and replication-blocking agents, respectively [7, 8]. Such hypersensitivity is similar to that of mammalian mutants of *ATM* and dominant negative mutants of *ATR* [3, 4], indicating conserved functions among plants and mammals. However, counterparts of the signal transducers CHK1, CHK2 and p53 are absent in *Arabidopsis*, suggesting that plants deploy a unique system to transmit the DNA damage signal downstream.

We have previously reported that *Arabidopsis* SOG1 is a plant-specific transcription factor that governs gene transcription, cell cycle arrest and programmed stem-cell death in response to DNA damage, and maintains genomic stability [10, 11]. Although the functions of SOG1 are similar to those of mammalian p53, the two proteins' amino acid sequences are unrelated to each other (Fig. 1A). Therefore, it would be intriguing to establish how SOG1 function is controlled in response to DNA damage. Here we demonstrate that serine-glutamine motifs in SOG1 are phosphorylated in an ATM-dependent and ATR-independent manner in response to DSBs. This phosphoregulation is prerequisite to signal transduction triggered by DSBs, implying an essential role for the ATM–SOG1 pathway in plants.

RESULTS AND DISCUSSION

SOG1 localization in planta.

The *sog1-1* mutant was isolated as a suppressor of the γ-sensitive phenotype displayed by seeds defective for the repair endonuclease XPF; thus, the transcriptional response to DNA damage (assessed by monitoring the expression of two DNA repair-related genes, *BRCA1* and *RAD51A)* is impaired in *xpf-2 sog1-1* (Fig. S1) [11, 12]. To determine the localization of SOG1 protein in plants, we generated transgenic *Arabidopsis* plants carrying *pSOG1::SOG1-GUS*, in which the promoter and coding regions of *SOG1* are fused in-frame to the β-glucuronidase (GUS) reporter gene. The transgene could partially restore the abolished transcriptional response to DNA damage in *xpf-2 sog1-1*: expression of both *BRCA1* and *RAD51A* was stimulated by a DSB inducer, zeocin, in transgenic plants (Fig. S1). We observed strong GUS staining in meristematic tissues, such as the shoot and root apical meristems, and in lateral root primordia in four-day-old seedlings (Fig. 1B-E). Faint GUS staining was also

observed in the vasculature of young leaves and in the root stele (Fig. 1B, C, F). Because the tissues in which GUS staining was observed all have dividing cells [13], we conclude that SOG1 functions mainly in tissues displaying cell division activity.

We assessed the subcellular localization of SOG1 using transgenic plants carrying *pSOG1::SOG1-GFP*, which complemented the defective transcriptional response of *sog1-1* to zeocin (Fig. S1). As shown in Fig. 1G, SOG1-GFP protein was localized exclusively to the nucleus. In addition to the observation that *SOG1* mRNA level does not increase after ionizing radiation treatment [14], our analysis showed that neither intensity nor localization of the SOG1-GFP signal were affected by 100 μM zeocin treatment in five-day-old seedlings (Fig. S2). This indicates that SOG1 function is not controlled by protein accumulation or subcellular localization.

SOG1 is phosphorylated in response to DNA damage.

In mammals, the preferred target for phosphorylation by ATM and ATR is serine or threonine followed by glutamine (S/T-Q) [4]. Since SOG1 has five SQ motifs in its C-terminal region (Fig. 2A), we predicted that SOG1 would likewise be modified by ATM and/or ATR, and thereby activated, in response to DNA damage. To test this possibility, we first prepared polyclonal antibodies against SOG1, but their specificity was too low to detect endogenous SOG1. We therefore generated *Arabidopsis* transgenic plants expressing 10xMyc-tagged *SOG1* under its own promoter. The SOG1-Myc fusion protein was functional, since it complemented the defective transcriptional response of *sog1-1* to zeocin (Fig. S1).

Immunoblotting with anti-Myc antibody detected an 80-kDa protein in transgenic plants expressing *SOG1-Myc* but not in wild-type plants (Fig. 2B), indicating that the antibody properly recognizes the fusion protein. The discrepancy

between this molecular mass and the estimated value of 66 kDa may be due to the low pI (4.62) of SOG1-10xMyc. To investigate whether SOG1 is modified in response to DNA damage, seedlings expressing *SOG1-Myc* were unirradiated (0 Gy) or γ-irradiated at 50 Gy, and, one hour later, total protein was extracted from roots. Immunoblots of protein extract from unirradiated plants showed a slower-migrating band (band 'b') in addition to the 80-kDa protein (band 'a'), while in irradiated plants a third, more slowly-migrating band (band 'c') appeared (Fig. 2C). Similar results were also obtained by zeocin treatment, in a dose-dependent manner (Fig. S3). Bands b and c both disappeared when protein extracts were incubated with λ protein phosphatase (λPP), but not with λPP and its inhibitor (Fig. 2D). These results suggest that a small amount of SOG1 is phosphorylated even without genotoxic stress, and that part of the SOG1 population becomes hyperphosphorylated in response to DSBs. In mammals, p53 level is kept low under unstressed conditions by protein degradation, whereas it is raised under genotoxic stress conditions [15]. However, we could not see any substantial change of the SOG1-Myc level in immunoblotting upon γ-irradiation or zeocin treatment (Fig. 2C, Fig. S3), which is consistent with the result obtained for the SOG1-GFP fusion protein (Fig. S2). Therefore, unlike mammalian p53, SOG1 function is probably mainly controlled by phosphorylation, rather than by protein accumulation. We could detect the hyperphosphorylated SOG1 after one hour of γ-irradiation or zeocin treatment (Fig. 2C, Fig. S3), suggesting that rapid modification of this transcription factor is involved in the DNA damage response.

Hyperphosphorylation of SOG1 is dependent on ATM.

Both SOG1 and ATM are required for the transcriptional response following γ-irradiation, suggesting that these two proteins act in the same pathway [11, 14]. We

therefore examined whether SOG1 phosphorylation after zeocin treatment is altered in the *atm-2* mutant. In *atm-2* carrying *pSOG1::SOG1-Myc*, the transcript level of endogenous *SOG1* was similar to that in wild-type, but the level of *SOG1-Myc* transgene mRNA was markedly lower than that in wild-type plants expressing *SOG1-Myc* (Fig. S4). This may be because the *atm-2* line is heterozygous for the *SOG1-Myc* transgene. As a result, the protein level of SOG1-Myc was reduced in *atm-2*; thus, to detect the phosphorylated forms, we exposed the immunoblots for a longer period (Fig. 2E). We found that hyperphosphorylated SOG1 (band 'c') was missing in zeocin-treated *atm-2*, but that DSB-independent phosphorylation represented by band b was observed in both wild-type and *atm-2* (Fig. 2E, left panel). This result demonstrates that DNA damage-induced hyperphosphorylation of SOG1 is ATM-dependent, whereas the constitutive phosphorylation is attributable to another kinase, which is not associated with the DNA damage response. We also tested the *atr-2* mutant, and found that hyperphosphorylated SOG1 (band 'c') appeared in zeocin-treated seedlings (Fig. 2E, right panel), indicating that ATR does not play a major role in zeocin-induced SOG1 phosphorylation.

To examine whether SOG1 is also hyperphosphorylated in response to replication stress, we used the two replication-blocking agents hydroxyurea (HU; a ribonucleotide reductase inhibitor) and aphidicolin (an inhibitor of DNA polymerase α). SOG1 was not hyperphosphorylated after up to 24 h of HU treatment (Fig. S5). Aphidicolin treatment yielded a trace amount of hyperphosphorylated SOG1 (Fig. S5), which may be a consequence of DSBs that were indirectly induced by replication block. These results suggest that SOG1 is hyperphosphorylated in response to DSBs, but not to replication stress.

To elucidate the putative phosphorylation sites, we transformed the *sog1-1*

mutant with *SOG1-Myc* or *SOG1(5A)-Myc*, the latter of which encodes serine-to-alanine substitutions at all five SQ motifs. Hyperphosphorylated SOG1 (band 'c') was observed in zeocin-treated plants carrying *SOG1-Myc* but not *SOG1(5A)-Myc* (Fig. 2F), indicating that one or more of the SQ motifs in the C-terminal region are targets for ATM-dependent phosphorylation. In contrast, band b was detected for both *SOG1-Myc* and *SOG1(5A)-Myc* regardless of zeocin treatment (Fig. 2F), showing that DSB-independent phosphorylation of SOG1 does not involve the SQ motifs.

Human ATM phosphorylates the SQ motifs of SOG1 *in vitro*.

Human ATM (hATM) phosphorylates p53 *in vitro*, and this kinase activity is markedly enhanced after treatment of cells with a radiomimetic drug [16]. Because the phosphatidylinositol-3 kinase domain of *Arabidopsis* ATM shares 67% amino acid similarity with that of hATM [17], we investigated whether ATM directly phosphorylates SOG1. Since we did not have a satisfactory antibody against *Arabidopsis* ATM, we immunoprecipitated endogenous hATM from human lymphoblastoid cells using a commercial anti-ATM antibody. For the kinase assay, the hATM immunoprecipitates were incubated with recombinant GST-SOG1 or GST-p53 as substrate. As expected, GST-p53 was phosphorylated by hATM, and higher phosphorylation was observed for hATM from cells that had been activated by γ-irradiation (Fig. S6A, lanes 1 and 2). Similarly, GST-SOG1 was phosphorylated by the hATM immunoprecipitates, and the phosphorylation level was also elevated by γ-irradiation, although the enhancement was not as marked as for GST-p53 (Fig. S6A, lanes 3 and 4). No phosphorylation was observed when GST-SOG1 was incubated with immunoprecipitates prepared using IgG, or when GST-SOG1(5A) carrying the

serine-to-alanine substitutions was incubated with the hATM immunoprecipitates (Fig. S6A, lanes 5 and 6). However, the phosphorylation was observed when GST-SOG1(3A) (with 350Ala, 356Ala and 372Ala) or GST-SOG1(2A) (with 430Ala and 436Ala) was used as substrate (Fig. S6C), indicating that multiple SQ sites are direct targets of hATM. The phosphorylation level of GST-SOG1(3A) or (2A) was much higher than that of GST-SOG1(WT). Since GST forms a dimer under physiological conditions [18], GST-SOG1(WT) may not be effectively phosphorylated due to altered conformation; conversely, alanine substitutions may render GST-SOG1(3A) or (2A) more easily accessible to hATM.

The SQ phosphorylation is required for SOG1 function.

To reveal the physiological significance of DNA damage-induced phosphorylation of SOG1, we tested the ability of *SOG1(5A)-Myc* to complement the phenotype of *sog1-1*. *SOG1-Myc* suppressed the γ-resistant leaf phenotype of the *xpf-2 sog1-1* mutant, which is defective in programmed developmental arrest upon DNA damage [12]; in contrast, *SOG1(5A)-Myc* could not complement this phenotype at all (Table 1). Similarly, transcriptional induction of *BRCA1* and *RAD51A* upon zeocin treatment was restored in *sog1-1* carrying *SOG1-Myc* but not *SOG1(5A)-Myc* (Fig. 3A). It is known that DSBs lead to SOG1-dependent cell death in the stem cell region of roots (Fig. 3B, arrowhead) [10]. Our observation of zeocin-treated roots showed that *SOG1-Myc* but not *SOG1(5A)-Myc* rescued the impaired cell death phenotype in *sog1-1* (Fig. 3B). Taken together, these results lead us to conclude that ATM-dependent phosphorylation of the SQ motifs is essential for SOG1 to exert its function in cell cycle arrest, the transcriptional response, and cell death induction in response to DSBs. The SQ motifs reside in the transcription activation domain of

SOG1 (Fig. 1A) [19]; thus, it is possible that phosphorylation of this domain affects the transcription-inducing activity of SOG1 or its interaction with cofactors that control the affinity and/or selectivity of SOG1 for target genes.

Although sensor proteins (ATM and ATR) for DNA damage are conserved between mammals and plants, the transcription factors (p53 and SOG1) that transmit the signals to downstream regulators have diverged. However, here we report the remarkable functional similarity that both p53 and SOG1 are phosphoregulated by ATM [16]. p53 is also known to be phosphorylated and activated by CHK2 [20]; although plants have no CHK2 homolog, our results show that SOG1 is constitutively phosphorylated by an unknown kinase, and that this phosphorylation is independent of DNA damage, ATM or the SQ motif. Further studies should reveal how kinase(s) other than ATM control SOG1 function in contexts such as development and the stress response.

The growth strategies of animals and plants are quite different; for example, plant cells have rigid cell walls, and therefore cannot migrate. Such differences have probably resulted in specific adjustments to their DNA damage response. We previously demonstrated that, in the epidermal cells of *Arabidopsis* root tips, DSBs induce an early onset of DNA polyploidization that enables meristematic cells to stop cell division and promotes cell expansion [21]. The inability of cells to migrate may require damaged cells to avoid the strategy of apoptosis, available to animal cells, because, in plants, dead cells are usually not replaced by the surrounding living cells. On the other hand, DSBs induce cell death in the stem cell region of *Arabidopsis* roots where the space left by dead cells can be occupied by new cells generated as the surrounding cells divide [22]. Because SOG1 is required for both DNA polyploidization and cell death in roots [11, 20], it is likely to regulate different sets of

target genes in a cell type-specific manner. It will be interesting to reveal how SOG1 phosphorylation is involved in the differential control of target genes and triggers various outputs, such as DNA repair, DNA polyploidization and cell death, to overcome genotoxic stress.

METHODS

Plant materials and growth conditions

Arabidopsis thaliana ecotype Columbia (Col) was used as the wild-type strain. *xpf-2*, *sog1-1*, *xpf-2 sog1-1, atm-2* (SALK_006953) and *atr-2* (SALK_032841) have been described previously [7, 8, 11]. Plants were grown on soil or MS media (1 x Murashige & Skoog (MS) salts including vitamins, 2% (w/v) sucrose, pH 6.0; 0.8% (w/v) gellangum agar for solid medium) under continuous light conditions at 23°C. Methods for the generation of transgenic plants and complementation tests are available in the supplementary information online.

RT-PCR

Total RNA was extracted from root tips of five-day-old seedlings using an RNeasy Plant Mini Kit (QIAGEN) according to the manufacturer's instructions. cDNA was synthesized from 0.8 μg of total RNA using Transcriptor Universal cDNA Master (Roche), and used as template for PCR amplification with specific primers. Detailed methods are available in the supplementary information online.

Immunoblotting

Proteins were separated in 8% SDS-polyacrylamide gels and blotted onto PVDF membranes. SOG1-Myc was detected using anti-Myc antibody (Santa Cruz). Phosphorylated SOG1-Myc was detected by Phos-tag reagent (NARD Institute). Detailed methods are available in the supplementary information online.

GUS staining and kinase assay

See the supplementary information online for details.

ACKNOWLEDGEMENTS

We are grateful to A. B. Britt (UC Davis) for critical reading of the manuscript. We thank H. Tatebe (NAIST) for helpful discussions and advice. Thanks go to C. Suga for isolating transgenic plants, to Y. Okushima (NAIST) for discussions and to I. Smith for refining the English. This work was supported by JSPS KAKENHI (Grants-in-Aid for Young Scientists (B)) (21770047 and 23770207 to K.O.Y., 24770045 to Minako U.), MEXT KAKENHI (Grant-in-Aid for Scientific Research on Innovative Areas) (24113514 to Minako U., 22119009 to Masaaki U.), the Kato Memorial Bioscience Foundation, and JST, CREST.

CONFLICT OF INTEREST

The authors declare that they have no conflict of interest.

AUTHOR CONTRIBUTIONS:

K.O.Y. planned the experiments and performed the majority of the experiments. J.K. performed the kinase assay. N.O. performed site-directed mutagenesis to generate alanine substitutions in GST-SOG1. Minako U. generated transgenic plants. K.O.Y., S.K., H.M. and Masaaki U. conceived the project and wrote the paper.

References

1. Ciccia A, Elledge SJ (2010) The DNA damage response: making it safe to play with knives. *Mol Cell* **40:** 179-204

2. Sancar A, Lindsey-Boltz LA, Unsal-Kacmaz K, Linn S (2004) Molecular mechanisms of mammalian DNA repair and the DNA damage checkpoints. *Annu Rev Biochem* **73:** 39-85

3. Flynn RL, Zou L (2011) ATR: a master conductor of cellular responses to DNA replication stress. *Trends Biochem Sci* **36:** 133-140

4. Bensimon A, Aebersold R, Shiloh Y (2011) Beyond ATM: the protein kinase landscape of the DNA damage response. *FEBS Lett* **585:** 1625-1639

5. Cheng Q, Chen J (2010) Mechanism of p53 stabilization by ATM after DNA damage. *Cell Cycle* **9:** 472-478

6. Smith J, Tho LM, Xu N, Gillespie DA (2010) The ATM-Chk2 and ATR-Chk1 pathways in DNA damage signaling and cancer. *Adv Cancer Res* **108:** 73-112

7. Garcia V, Bruchet H, Camescasse D, Granier F, Bouchez D, Tissier A (2003) AtATM is essential for meiosis and the somatic response to DNA damage in plants. *Plant Cell* **15:** 119-132

8. Culligan K, Tissier A, Britt A (2004) ATR regulates a G2-phase cell-cycle checkpoint in *Arabidopsis thaliana*. *Plant Cell* **16:** 1091-1104

9. Abraham RT (2001) Cell cycle checkpoint signaling through the ATM and ATR kinases. *Genes Dev* **15:** 2177-2196

10. Furukawa T, Curtis MJ, Tominey CM, Duong YH, Wilcox BW, Aggoune D, Hays JB, Britt AB (2010) A shared DNA-damage-response pathway for induction of stem-cell death by UVB and by gamma irradiation. *DNA Repair (Amst)* **9:** 940-948

11. Yoshiyama K, Conklin PA, Huefner ND, Britt AB (2009) Suppressor of

gamma response 1 (*SOG1*) encodes a putative transcription factor governing multiple responses to DNA damage. *Proc Natl Acad Sci U S A* **106:** 12843-12848

12. Preuss SB, Britt AB (2003) A DNA-damage-induced cell cycle checkpoint in *Arabidopsis*. *Genetics* **164:** 323-334

13. Beck CB (2010) An introduction to Plant Structure and Development. *Cambridge University Press* **Second edition**

14. Culligan KM, Robertson CE, Foreman J, Doerner P, Britt AB (2006) ATR and ATM play both distinct and additive roles in response to ionizing radiation. *Plant J* **48:** 947-961

15. Kruse JP, Gu W (2009) Modes of p53 regulation. *Cell* **137:** 609-622

16. Lavin MF, Scott SP, Kozlov S, Gueven N (2004) Analyzing the regulation and function of ATM. *Methods Mol Biol* **281:** 163-178

17. Garcia V, Salanoubat M, Choisne N, Tissier A (2000) An ATM homologue from *Arabidopsis thaliana*: complete genomic organisation and expression analysis. *Nucleic Acids Res* **28:** 1692-1699

18. Liew CK, Gamsjaeger R, Mansfield RE, Mackay JP (2008) NMR spectroscopy as a tool for the rapid assessment of the conformation of GST-fusion proteins. *Protein Sci* **17:** 1630-1635

19. Jensen MK, Kjaersgaard T, Nielsen MM, Galberg P, Petersen K, O'Shea C, Skriver K (2010) The *Arabidopsis thaliana* NAC transcription factor family: structure-function relationships and determinants of ANAC019 stress signalling. *Biochem J* **426:** 183-196

20. Shieh SY, Ahn J, Tamai K, Taya Y, Prives C (2000) The human homologs of checkpoint kinases Chk1 and Cds1 (Chk2) phosphorylate p53 at multiple DNA damage-inducible sites. *Genes Dev* **14:** 289-300

21. Adachi S *et al* (2011) Programmed induction of endoreduplication by DNA double-strand breaks in *Arabidopsis*. *Proc Natl Acad Sci U S A* **108:** 10004-10009

22. Fulcher N, Sablowski R (2009) Hypersensitivity to DNA damage in plant stem cell niches. *Proc Natl Acad Sci U S A* **106:** 20984-20988

Table 1. Phosphorylation of the SQ motif is required for γ-sensitive growth in *xpf-2*.

Line	Genotype	Total	No. γ-resistant (*xpf-2 sog1-1* phenotype)	No. γ-sensitive (*xpf-2 SOG1* phenotype)	% γ-sensitive
KS12	wild-type	35	35	0	0
KO711	*xpf-2*	23	0	23	100
KO735	*xpf-2 sog1-1*	44	44	0	0
KS90	*xpf-2 sog1-1/SOG1-Myc*	32	3	29	91
KS70	*xpf-2 sog1-1/SOG(5A)-Myc*	31	31	0	0

Imbibed seeds were γ-irradiated (100 Gy), and grown on MS plates for 10 days. The number of plants that were γ-resistant (plants having one or more true leaves) and γ-sensitive (plants with no true leaves) was scored by eye. If a transgene is functional, the γ-sensitive (*xpf-2 SOG1*) phenotype appears. Note that all unirradiated seedlings formed true leaves.

Figure Legends

Figure 1. Expression pattern of SOG1.

(A) Functional domains of p53 and SOG1. Ser 15 and Ser 20 in p53 are phosphorylated in response to DNA damage. Serine residues of the five SQ motifs in the C-terminal region of SOG1 are shown. (B)-(F) GUS staining of four-day-old seedlings expressing *pSOG1::SOG1-GUS*. Whole seedlings (B), cotyledon (C), root tip (D), lateral root primordium (E), and root stele (F). (G) Microscopic observation of GFP fluorescence in a four-day-old root tip expressing *pSOG1::SOG1-GFP*. The root was counterstained with propidium iodide to visualize the cell wall. The inset shows a magnified image of the indicated region. Scale bars, 1 mm (B and C) and 0.1 mm (D-G).

Figure 2. *In vivo* phosphorylation of SOG1.

(A) Amino acid sequence of SOG1. Blue and red letters show the NAC domain and the SQ motifs, respectively. (B) Immunoblotting of total protein with anti-Myc antibody (upper panel). Total protein was extracted from wild-type seedlings (WT) and transgenic plants expressing *pSOG1::SOG1-Myc* (WT/*SOG1-Myc*). As a control, the same membrane was incubated with anti-CDKA;1 antibody (lower panel). (C, D) Plants harboring *pSOG1::SOG1-Myc* were untreated (0 Gy) or treated with γ-irradiation (50 Gy), and total protein was extracted an hour later. Total protein was incubated with λ protein phosphatase (λPP) in the presence or absence of phosphatase inhibitor (D). '-' indicates controls without λPP. Phosphorylated forms of SOG1 were detected in an SDS-PAGE gel containing Phos-tag. The exposure time was 10 or 40 sec in (D). (E, F) Plants harboring *pSOG1::SOG1-Myc* or *pSOG1::SOG1(5A)-Myc* were used. Five-day-old seedlings grown on MS plates were transferred to liquid

medium with (+) or without (-) 1 mM zeocin, and total protein was extracted an hour later. The protein extracts were separated in an SDS-PAGE gel containing Phos-tag. To ensure that transferring seedlings from solid to liquid had no effect on SOG1 phosphorylation, total protein was also extracted from seedlings on MS plates as a non-transferred control (n.t.). In the right panel of (E), five times more total protein was used for *atm-2* and *atr-2* than for wild-type to obtain comparable loading of SOG1-Myc. Coomassie blue staining is displayed below. Non-phosphorylated, phosphorylated and hyperphosphorylated SOG1-Myc (bands a, b and c, respectively) are indicated by arrowheads.

Figure 3. SQ motif phosphorylation is required for SOG1 function.

(A) Semiquantitative RT-PCR of *BRCA1* and *RAD51A*. Five-day-old wild-type, *sog1-1*, and *sog1-1* carrying *pSOG1::SOG1-Myc* or *pSOG1::SOG1(5A)-Myc* were transferred to fresh MS liquid medium containing 0 (-) or 100 μM (+) zeocin, and RNA was extracted from root tips 2 h later. As a control, cDNA for *eIF4A1* (eukaryotic initiation factor 4A) was amplified. (B) Stem cell death in zeocin-treated root tips. Four-day-old seedlings were transferred to a new MS plate containing 0 or 100 μM zeocin, and roots were stained with propidium iodide 24 h later. Arrowheads indicate cell death in the stem cell region. Bar, 100 μm.

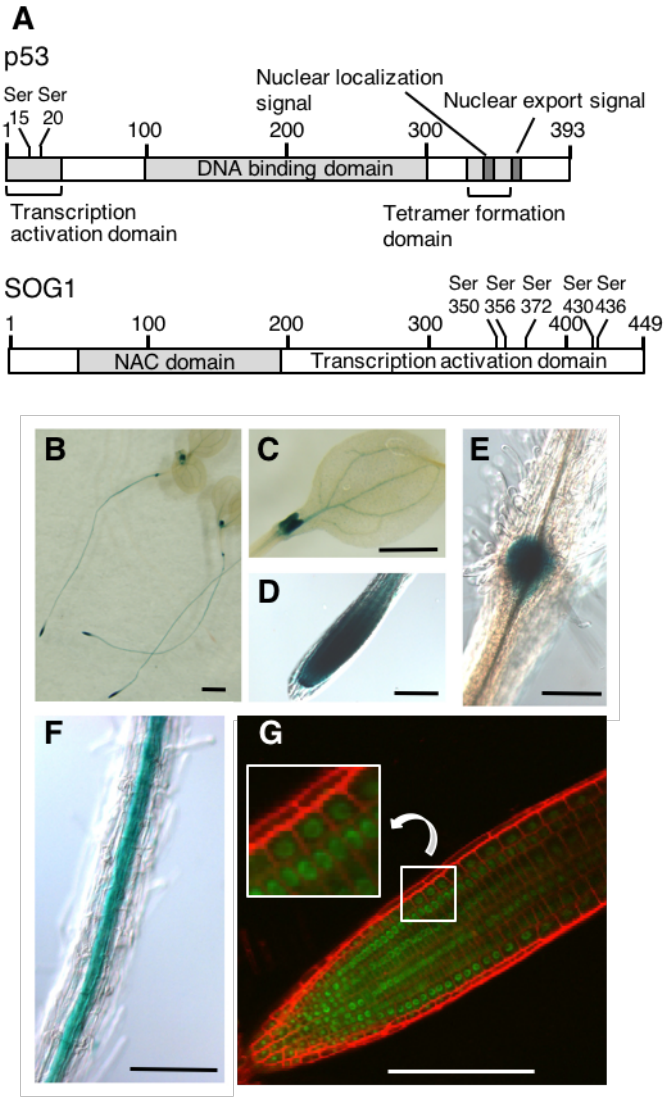
A
p53
Ser Ser
15 20
Nuclear localization
signal
Nuclear export signal
1
100
200
300
393
DNA binding domain
Transcription
activation domain
Tetramer formation
domain
SOG1
Ser Ser Ser Ser Ser
350 356 372 430 436
1
100
200
300
400
449
NAC domain
Transcription activation domain
B
C
D
E
F
G

Figure 1

A

MAGRSWLIDSNRIATKIMSASASSDPRQVVWKSNPSRHCPKCQHVIDNSDVVDDWPGLPRGVKFDPSDPEIIWHLL
AKSGLSGLSSHPFIDEFIPTVNQDDGICYTHPKNLPGVKSDGTVSHFFHKAIKAYSTGTRKRRKIHDDDFGDVRWH
KTGRTKPVVLDGVQRGCKKIMVLYGGKAVKTNWVMHQYHLGIEEDEKEGDYVVSKIFYQQPQQLVVKRGDKAEQEV
SEDIFAAVTPTADPVTPKLATPEPRNAVRICSDSHIASDYVTPSDYVSAHEVSLAETSEVMCMEDEVQSIQPNHER
PSSGPELEHGLENGAKEMLDDKEEQEKDRDNENQGEEDPTWFDSGSQFILNSQQLVEALSLCDDLLGSQDREENTN
SGSLKDKQPCIADYAHLGPEDFKRDLEECQKIVLDPSNIELDTPPEFRLSQLEFGSQDSFLAWGTGKTD

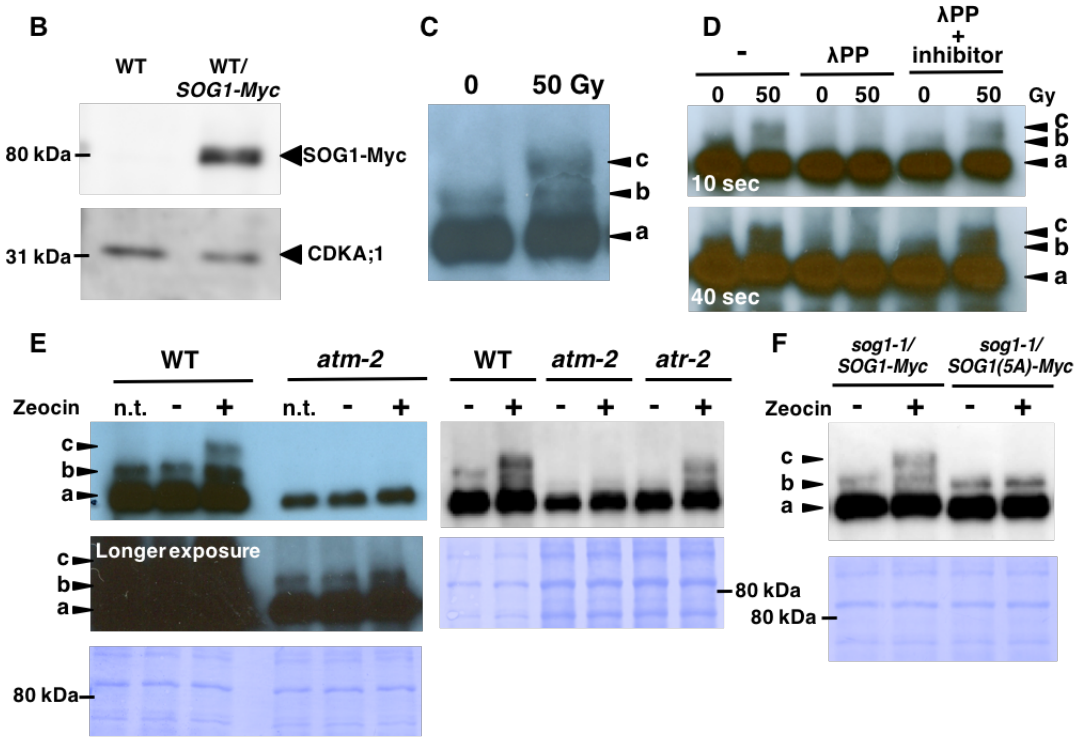

Figure 2

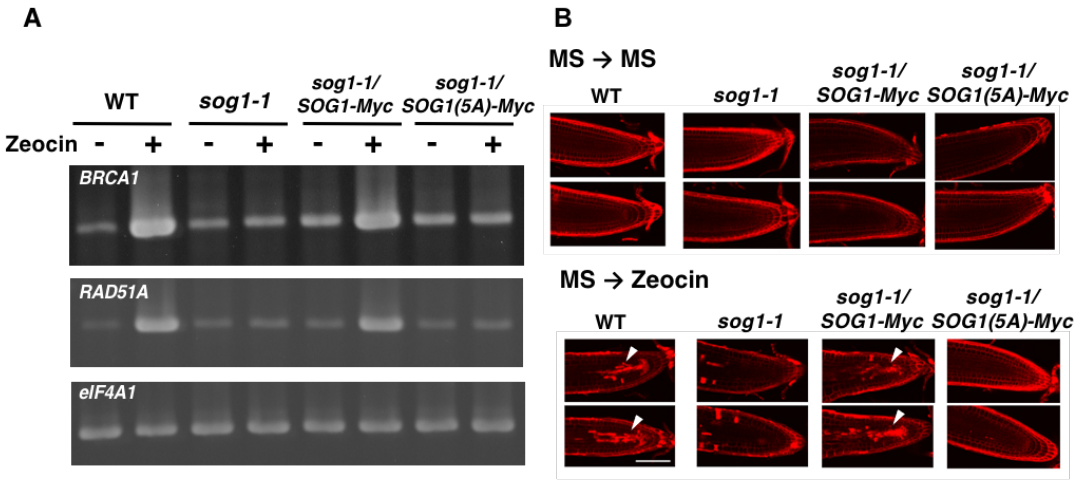
A
WT
sog1-1
sog1-1/ SOG1-Myc
sog1-1/ SOG1(5A)-Myc
Zeocin - + - + - + - +
BRCA1
RAD51A
eIF4A1
B
MS → MS
WT
sog1-1
sog1-1/ SOG1-Myc
sog1-1/ SOG1(5A)-Myc
MS → Zeocin
WT
sog1-1
sog1-1/ SOG1-Myc
sog1-1/ SOG1(5A)-Myc

Figure 3

Supplementary information

Plant materials and growth conditions

Arabidopsis thaliana ecotype Columbia (Col) was used as the wild-type strain. *xpf-2*, *sog1-1*, *xpf-2 sog1-1*, *atm-2* (SALK_006953), and *atr-2* (SALK_032841) have been described previously [1-3]. Plants were grown on soil or MS media (1 x Murashige & Skoog (MS) salts including vitamins, 2% (w/v) sucrose; pH 6.0; 0.8% (w/v) gellangum agar for solid medium) under continuous light conditions at 23°C. Five-day-old seedlings on MS plates were irradiated using a ^{137}Cs source (Radiation Biology Center, Kyoto University), with doses ranging from 0 to 100 Gy and at a rate of 1.1 Gy/min. Zeocin (Invitrogen) was used as a DNA double-strand break inducer. Hydroxyurea (Wako) and aphidicolin (Wako) were used as replication-blocking agents.

Generation of transgenic lines

To prepare various protein fusion constructs, we used the same genomic DNA fragment, comprising the SOG1 ORF and 1840 bp of upstream sequence, as we reported previously for complementation testing [3]. To generate the native promoter-driven SOG1-GUS, SOG1-GFP, and SOG1-Myc constructs, this fragment was amplified, by PCR using KOD-Plus-polymerase (TOYOBO), from *Arabidopsis* Col genomic DNA using the primers G25580F11 and G25580R11. Purified PCR products were subcloned into the pENTR/D-TOPO vector (Invitrogen) according to the manufacturer's instructions. Each fragment was then cloned into pGWB3 (no promoter, C-GUS), pGWB4 (no promoter, C-GFP), or pGWB19 (no promoter, C-10xMyc) binary plasmids [4] with LR clonase (Invitrogen) to generate SOG1 protein fusion constructs with *GUS, GFP or Myc*. These were introduced into *A.*

thaliana via *Agrobacterium tumefaciens (GV3101)*-mediated floral-dip transformation [5]. Transformants with a single insertion were selected based on kanamycin resistance. Primer sequences are listed in Supplemental Table 1.

GUS staining

Four-day-old wild-type seedlings carrying *pSOG1::SOG1-GUS* were incubated in 90% (v/v) acetone at 4°C for 15 min, and washed in 100 mM sodium phosphate buffer (pH 7.0). Samples were incubated in a GUS staining buffer (100 mM sodium phosphate, 3 mM EDTA, 0.05% (v/v) Triton X-100, 5 mM potassium ferricyanide, and 0.5 mg/ml 5-bromo-4-chloro-3-indolyl-β-D-glucuronide (pH 7.0)) at 37°C for 1 h. After staining, the plants were washed with 70% ethanol at room temperature. The seedlings were mounted in 50% (w/v) glycerol and visualized under a microscope.

Analysis of subcellular localization

Five-day-old wild-type seedlings carrying *pSOG1::SOG1-GFP* were transferred to an MS plate with or without 100 μM zeocin, and GFP fluorescence was observed 0.5, 2, 7 and 24 h later. Roots were counterstained with 10 μg/ml propidium iodide (PI). GFP and PI signals were observed with a confocal laser scanning microscope (Olympus FV1000 or Leica TCS SP2).

Complementation test

To determine whether the transgenes *pSOG1::SOG1-GUS*, *pSOG1::SOG1-GFP*, *pSOG1::SOG1-Myc, and pSOG1::SOG1(5A)-Myc* were functional, we performed complementation tests in T3 homozygous lines by looking for transcriptional up-regulation of *BRCA1* and *RAD51A* in response to DNA damage, as described

previously [3].

RT-PCR

Five-day-old seedlings of wild-type, *xpf-2 sog1-1,* and *sog1-1* carrying *pSOG1::SOG1-GUS*, *pSOG1::SOG1-GFP*, *pSOG1::SOG1-Myc* or *pSOG1::SOG1(5A)-Myc* were transferred to MS liquid medium containing 0 or 100 μM zeocin, and after a 2-h incubation, RNA was extracted from root tips (RNeasy Plant Mini Kit; QIAGEN). RNA samples were treated with DNase (RNase-Free DNase Set; QIAGEN) and quantified. To produce cDNA for RT-PCR, 0.8 μg of total RNA from each condition described above was reverse-transcribed, using random hexamer primers and a Transciptor Universal cDNA Master (Roche), in a 10-μl reaction according to the manufacturer's protocol. RT-PCR was performed in 10-μl reactions using Ex-Taq polymerase (TaKaRa) and the following gene-specific primers: eIF4A-1 and eIF4A-5 for *eIF4A1*, brca1F2 and brca1rtR2 for *BRCA1*, rad51AF1 and rad51ArtR1 for *RAD51A,* 25580F15 and 25580R4 for endogeneous *SOG1*, and 25580F13 and mycR1 for the transgene *SOG1-Myc*. PCR-cycle parameters for all primer pairs were 30 s at 95°C, 30 s at 62°C, and 60 s at 72°C: 25 cycles. *eIF4A1* (eukaryotic initiation factor 4A1) served as a standard for RT-PCR amplification. Primer sequences are listed in Supplemental Table 1.

Immunoblotting

Root tips were excised and ground in the following buffer: 10 mM Tris (pH 7.6), 150 mM NaCl, 2 mM EDTA, 0.5% (v/v) Nonidet P-40 (Nakalai Tesque), 1 mM DTT, and protease inhibitor cocktail (Sigma). The slurry was centrifuged twice to remove debris, and the supernatant was recovered and used for subsequent analysis. Proteins (1 μg)

were loaded onto an 8% SDS–polyacrylamide gel for electrophoresis. After electrophoresis, the proteins were electroblotted to a polyvinylidene difluoride (PVDF) membrane (Millipore) in the following buffer: 6.3 mM $NaHCO_3$, 4.3 mM Na_2CO_3, pH 9.5, and 20% methanol. The membrane was then incubated for 2 h at room temperature in anti-Myc primary antibody A-14 (Santa Cruz, 1:2000 dilution), rinsed 3 times with 1 x TBST, and incubated with anti-rabbit immunoglobulin horseradish peroxidase-linked secondary antibody (Promega, 1:4000) to detect SOG1-Myc. The membrane was washed as before and exposed to X-ray film or processed with a luminescent image analyzer (LAS-1000, FUJIFILM) after incubation with enhanced chemiluminescence reagents (ECL Prime) (GE Healthcare). Phos-tag reagent (NARD Institute) was used for the phospho protein mobility shift assay to detect phosphorylated SOG1 protein. Phosphorylated proteins are visualized as bands migrating more slowly than those of non-phosphorylated proteins [6]. Proteins were separated in an 8% SDS-PAGE gel containing 20 μM Phos-tag and 40 μM $MnCl_2$. λ protein phosphatase (λPP) was used to test for phosphorylated SOG1. Protein lysate was incubated at 30°C for 2.5 h in 15 μl of 1 x λPP buffer containing 80 U of λPP (New England BioLabs), and 1% Triton X-100. As a negative control experiment, phosphatase treatment was performed in $MnCl_2$-free phosphatase buffer in the presence of phosphatase inhibitor cocktail (0.1 mM Na_3VO_4, 1 mM NaF, 60 mM β-glycerophosphatase, 20 mM p-nitrophenylphosphate).

Multiple site-directed mutagenesis

To generate a SOG1 mutant devoid of SQ motif(s), we performed multiple site-directed mutagenesis [7], and confirmed the changes by sequencing. iProof polymerase (BIO-RAD) was used for the site-directed reaction with the following

primers: for SOG1 cDNA, 25580F15, 25580(S->A)R16, 25580(S->A)R17, and 25580(S->A)R18; for SOG1 genomic DNA, 25580F15, 25580(S->A)R16, 25580(S->A)R17, 25580(S->A)R19, and 25580(S->A)R20. SOG1(5A) indicates that all five SQ motifs (Ser-Gln) of SOG1 are mutated to AQ (Ala-Gln). Primer sequences are listed in Supplemental Table 1.

ATM kinase assay

SOG1 cDNA was amplified by PCR using KOD-Plus-polymerase (TOYOBO), with SOG1 cDNA plasmid obtained from ABRC (https://abrc.osu.edu/) as template and the primers G25580F10 and G25580R10. Purified PCR products were subcloned into the pENTR/D-TOPO vector (Invitrogen) according to the manufacturer's instruction. Each fragment was then cloned into pDEST15 (T7 promoter-GST) plasmid (Invitrogen) with LR clonase (Invitrogen) to generate a SOG1 cDNA fusion construct with *GST*. GST-tagged SOG1 was purified using a GSTrap FF column (GE Healthcare) according to the manufacturer's instruction. Phosphorylation of GST-SOG1 by ATM was investigated with an ATM kinase reaction protocol, described previously [8]. ATM was immunoprecipitated with anti-ATM antibody (Calbiochem, PC116) after extraction from human lymphoblastoid cells that had been exposed to γ-irradiation (10 Gy). The precipitated ATM was resuspended in kinase buffer (10 mM HEPES-NaOH (pH 7.5), 50 mM NaCl, 10 mM $MgCl_2$, 10 mM $MnCl_2$, 100 mM Na_3VO_4, 1 mM DTT) containing 5 mM ATP, GST-SOG1 (wild type or mutants with alanine substitution(s)) or GST- $p53_{1-44}$ [9] and 370 kBq [γ-^{32}P]ATP (220 TBq/nmol; GE Healthcare). After incubation for 30 min at 30˚C, the samples were added to Laemmli buffer (2% SDS, 5% glycerol, 5% 2-mercaptoethanol, 0.1% bromophenol blue, 62.5 mM Tris-HCl [pH 6.8]), heated at 95˚C for 5 min, and

electrophoresed on a 10% SDS-polyacrylamide gel. The phosphorylated substrates were analyzed with BAS1500 (FUJIFILM).

1. Culligan K, Tissier A, Britt A (2004) ATR regulates a G2-phase cell-cycle checkpoint in *Arabidopsis thaliana*. *Plant Cell* **16:** 1091-1104

2. Garcia V, Bruchet H, Camescasse D, Granier F, Bouchez D, Tissier A (2003) AtATM is essential for meiosis and the somatic response to DNA damage in plants. *Plant Cell* **15:** 119-132

3. Yoshiyama K, Conklin PA, Huefner ND, Britt AB (2009) Suppressor of gamma response 1 (*SOG1*) encodes a putative transcription factor governing multiple responses to DNA damage. *Proc Natl Acad Sci U S A* **106:** 12843-12848

4. Nakagawa T *et al* (2007) Development of series of gateway binary vectors, pGWBs, for realizing efficient construction of fusion genes for plant transformation. *J Biosci Bioeng* **104:** 34-41

5. Clough SJ, Bent AF (1998) Floral dip: a simplified method for *Agrobacterium*-mediated transformation of *Arabidopsis thaliana*. *Plant J* **16:** 735-743

6. Kinoshita E, Kinoshita-Kikuta E, Takiyama K, Koike T (2006) Phosphate-binding tag, a new tool to visualize phosphorylated proteins. *Mol Cell Proteomics* **5:** 749-757

7. Sawano A, Miyawaki A (2000) Directed evolution of green fluorescent protein by a new versatile PCR strategy for site-directed and semi-random mutagenesis. *Nucleic Acids Res* **28:** E78

8. Kobayashi J, Kato A, Ota Y, Ohba R, Komatsu K (2010) Bisbenzamidine derivative, pentamidine represses DNA damage response through inhibition of histone H2A acetylation. *Mol Cancer* **9:** 34

9. Lavin MF, Scott SP, Kozlov S, Gueven N (2004) Analyzing the regulation and function of ATM. *Methods Mol Biol* **281:** 163-178

Supplementary Figure Legends

Figure S1. RT-PCR of *BRCA1* and *RAD51A* in transgenic plants.

Five-day-old seedlings of wild-type (WT), *xpf-2 sog1-1*, and *xpf-2 sog1-1* carrying *pSOG1::SOG1-GUS, pSOG1::SOG1-GFP* or *pSOG1::SOG1-Myc* were transferred to MS liquid medium containing 0 (-) or 100 μM (+) zeocin, and, after a 2-h incubation, RNA was extracted from root tips. The expression of *BRCA1* and *RAD51A* was analyzed by semiquantitative RT-PCR. *eIF4A1* (eukaryotic initiation factor 4A1) was used as a control.

Figure S2. Subcellular localization of SOG1-GFP in the presence of zeocin.

Five-day-old seedlings carrying *pSOG1::SOG1-GFP* were transferred to an MS plate with (lower panel) or without (upper panel) 100 μM zeocin, and GFP fluorescence was observed after 0.5, 2, 7 and 24 h. Roots were counterstained with propidium iodide. Insets are magnified images of the regions indicated by smaller white squares. Bar, 0.1 mm.

Figure S3. Zeocin-induced SOG1 phosphorylation.

Five-day-old seedlings carrying *pSOG1::SOG1-Myc* were transferred to liquid medium containing the indicated concentrations of zeocin for 1 h, and total protein was immunoblotted with anti-Myc antibody. Coomassie blue staining is displayed below.

Figure S4. RT-PCR of endogenous *SOG1* and *SOG1-Myc* transgene in *atm* and *atr* mutants.

Five-day-old seedlings of wild-type (WT), *atm-2* and *atr-2* carrying

pSOG1::SOG1-Myc were used for RNA extraction from root tips. The expression of endogenous *SOG1* and *SOG1-Myc* transgene was analyzed by semiquantitative RT-PCR. *eIF4A1* (eukaryotic initiation factor 4A1) was used as a control.

Figure S5. SOG1 is not hyperphosphorylated in response to replication stress.

Plants harboring *pSOG1::SOG1-Myc* were grown on MS plates, and five-day-old seedlings were transferred to liquid medium with or without 200 mM hydroxyurea (HU), 120 μg/ml aphidicolin (Aph), or 1 mM zeocin (Zeo). Total protein was extracted at the indicated time points and separated in an SDS-PAGE gel containing 25 μM Phos-tag. Immunoblotting was conducted with anti-Myc antibody. Coomassie blue staining is displayed below.

Figure S6. Human ATM phosphorylates SOG1 *in vitro*.

(A) Kinase assay of p53 and SOG1. Human ATM (hATM) was immunoprecipitated with anti-ATM antibody after treatment of human lymphoblastoid cells with or without γ-irradiation (10 Gy). As a control, IgG was used for immunoprecipitation. GST-p53, GST-SOG1 and GST-SOG1(5A) were used as substrate. Phosphorylated proteins were separated by SDS-PAGE and detected by autoradiography. (B) Coomassie blue staining of (A). (C) Kinase assay of SOG1 with alanine substitutions. Human ATM was immunoprecipitated from human lymphoblastoid cells with γ-irradiation (10 Gy). GST-SOG1(WT), GST-SOG1(5A) (with 350Ala, 356Ala, 372Ala, 430Ala and 436Ala), GST-SOG1(3A) (with 350Ala, 356Ala and 372Ala) and GST-SOG1(2A) (with 430Ala and 436Ala) were used as substrate. Coomassie blue staining is displayed below.

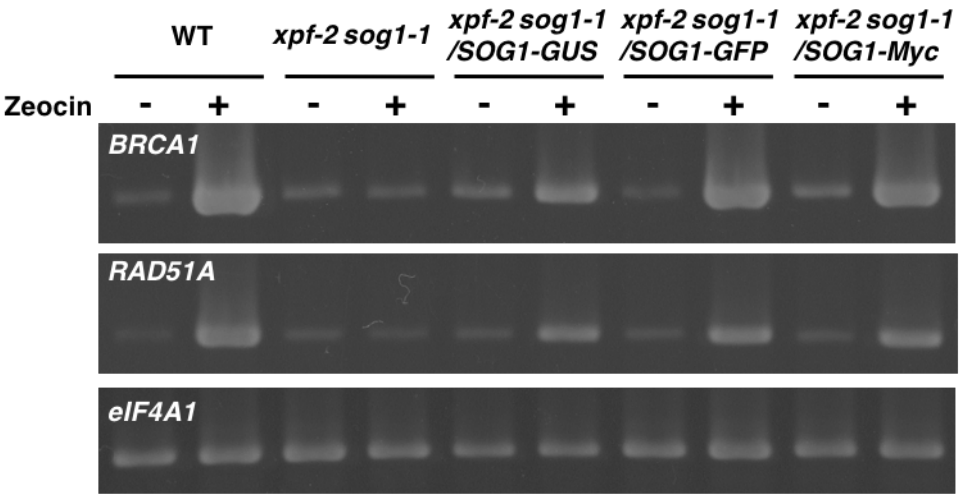
WT
xpf-2 sog1-1
xpf-2 sog1-1 /SOG1-GUS
xpf-2 sog1-1 /SOG1-GFP
xpf-2 sog1-1 /SOG1-Myc
Zeocin
- + - + - + - + - +
BRCA1
RAD51A
eIF4A1

Figure S1

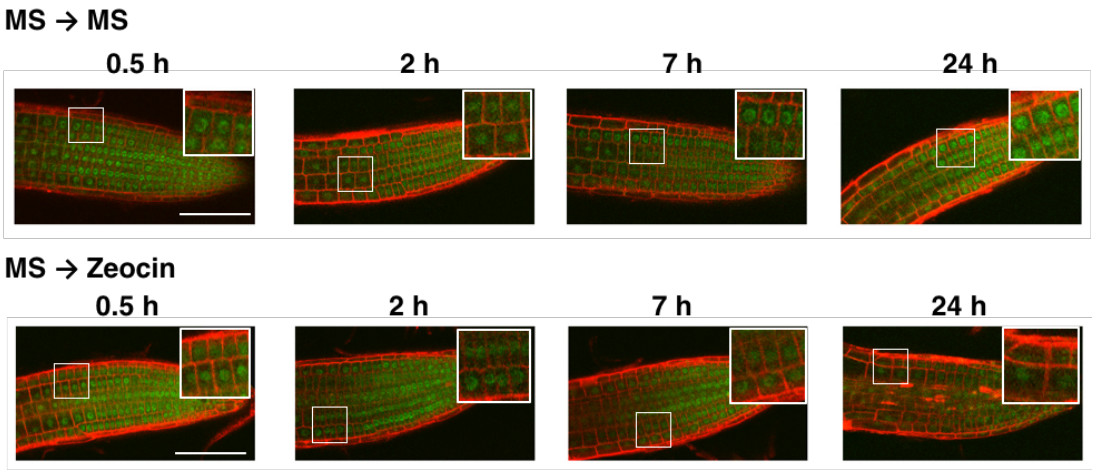

Figure S2

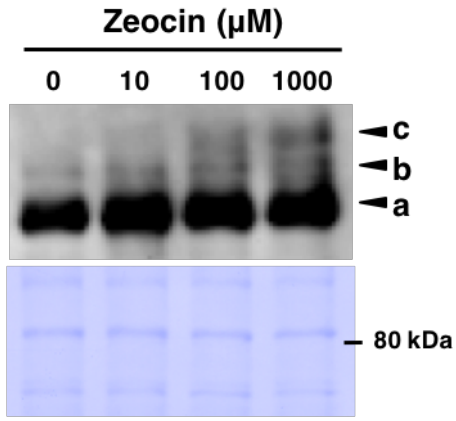

Figure S3

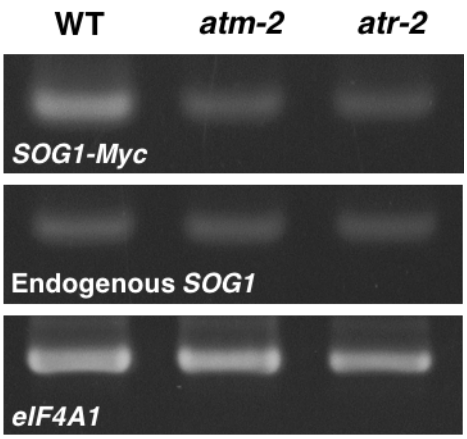

Figure S4

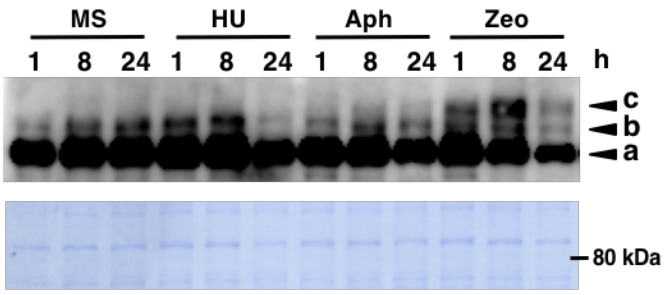

Figure S5

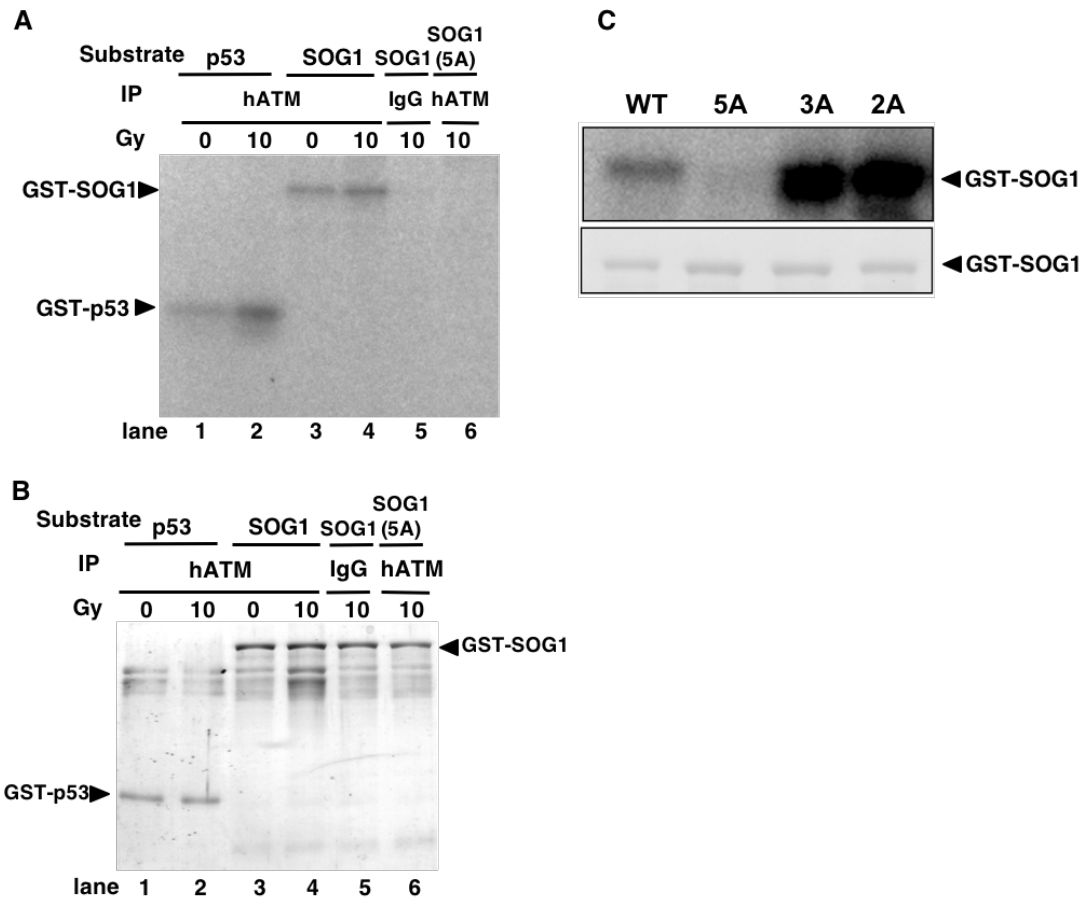
A
Substrate
p53
SOG1
SOG1
SOG1 (5A)
IP
hATM
IgG
hATM
Gy
0
10
0
10
10
10
GST-SOG1
GST-p53
lane
1
2
3
4
5
6
B
Substrate
p53
SOG1
SOG1
SOG1 (5A)
IP
hATM
IgG
hATM
Gy
0
10
0
10
10
10
GST-SOG1
GST-p53
lane
1
2
3
4
5
6
C
WT
5A
3A
2A
GST-SOG1
GST-SOG1

Figure S6

Supplementary Table

Table S1. Sequences of primers used in this study

Locus	Purpose	Name	Primer	Primer Nucleotide sequence
SOG1	Cloning	G25580F11	F	5'-AAAAAGCAGGCTTTCCCCGAGATGAAAGAATCAACTTCAAC-3'
		G25580R11	R	5'-AGAAAGCTGGGTTATCAGTCTTTCCAGTCCCCCAAGC-3'
	Cloning	G25580F10	F	5'-AAAAAGCAGGCTTTATGGCTGGGCGATCATGGCTG-3'
		G25580R10	R	5'- AGAAAGCTGGGTTTCAATCAGTCTTTCCAGTCCCCCAAG-3'
eIF4A1	RT-PCR	eIF4A-1	F	5'-CTCTCGCAATCTTCGCTCTTCTCTTT-3'
		eIF4A-5	R	5'-TCATAGATCTGGTCCTTGAAAC-3'
BRCA1	RT-PCR	brca1F2	F	5'- GGATGGGAAGAGAACTCAAGTGC -3'
		brca1rtR2	R	5'- GTTGCTCGTCTTCCTTCGATGG-3'
RAD51A	RT-PCR	rad51AF1	F	5'- GGTGTTGCTTATACTCCGAGGAAGG-3'
		rad51ArtR1	R	5'- CAGCCACACCAAACTCATCTGCTAAC -3'
SOG1	RT-PCR	25580F15	F	5'-ATGATGGAATCTGTTACACTCATCC-3'
		25580R4	R	5'-CAGAACTTGGTCTTTCATGATTAGG-3'
SOG1-Myc	RT-PCR	25580F13	F	5'-ACTTCAAACGTGATCTGGAGG-3'
		mycR1	R	5'-TAGCTTTTGTTCACCGTTAATTAACC-3'
SOG1	site-directed	25580F15	F	5'-ATGATGGAATCTGTTACACTCATCC-3'
		25580(S->A)R16	R	5'-CACAAGCTGTTGCGCATTCAAGATAAACTGAGCTCCACTGTCAA-3'
		25580(S->A)R17	R	5'-GTTTTCCTCCCTGTCCTGTGCTCCCAAGAGATCG-3'
		25580(S->A)R18	R	5'-GCTGTCCTGTGCTCCAAATTCCAGCTGGGCCAGACGAAACTCAG-3'
		25580(S->A)R19	R	5'-CTAAGCTTACCAGCTGGGCCAGACGAAACTCAGG-3'
		25580(S->A)R20	R	5'-GCGAGAAAGCTGTCCTGTGCTCCAAATTCCTAAACACAG-3'